An Iterative Radiative Transfer Code For Ocean–Atmosphere Systems

ZIAUDDIN AHMAD

Systems and Applied Sciences Corporation, Riverdale, MD 20840

ROBERT S. FRASER

NASA/Goddard Space Flight Center, Laboratory for Atmospheric Sciences, Greenbelt, MD 20771

(Manuscript received 20 January 1981, in final form 4 November 1981)

ABSTRACT

We describe the details of an iterative radiative transfer code for computing the intensity and degree of polarization of diffuse radiation in models of the ocean–atmosphere system. The present code neglects the upwelling radiation from below the ocean surface and as such is applicable to the part of the spectrum where the absorption by water is strong. To establish the reliability of our numerical scheme as well as the computer code, we compare our results with those of Fraser and Walker (1968), Dave (1972) and Mullamaa (1964) and find them to be in excellent agreement. We also obtained reasonably good qualitative agreement with Plass *et al.* (1975) who utilize the Monte Carlo technique to solve the radiative transfer equation for the ocean–atmosphere system. Our computations also show that both the intensity as well as the degree of polarization of the upwelling diffuse radiation at the top of the atmosphere vary significantly, when the rough ocean at the base of the atmosphere is replaced by a Lambertian surface that reflects the same energy as the rough ocean.

1. Introduction

In almost all of the earth-orbiting satellite experiments which are of interest to meteorologists, environmentalists, and others, one measures the intensity of the upwelling diffuse radiation leaving the top of the atmosphere in the nadir direction or a set of nadir angles. These intensities carry valuable information about the atmosphere and the underlying surface at the base of the atmosphere and hence provide a means to study the ocean, the earth and its atmosphere, globally. However, to understand the characteristics of the radiation leaving the top of the atmosphere and extract information, particularly when the satellite is over the ocean, it is important that the radiation is investigated with the aid of a realistic ocean–atmosphere model with proper reflection laws at the lower boundary and accounting for all orders of scattering and polarization. Most of the existing realistic atmospheric models assume a Lambertian reflector at the lower boundary of the atmosphere. These models give erroneous results when applied to cases where the lower boundary is known to reflect light anisotropically.

Earlier Fraser and Walker (1968) reported the intensity and degree of polarization for a simple model of the ocean–atmosphere system, which consisted of a standard gas and rested on a smooth ocean surface. Later Dave (1972) and Kattawar *et al.* (1973) developed radiative transfer codes to compute both the intensity and degree of polarization of the diffuse radiation for models of the ocean–atmosphere system where the lower boundary was still a smooth surface, but the atmosphere could be vertically inhomogeneous and could include an absorbing gas, aerosols and standard gas. Raschke (1972), Plass *et al.* (1975) and most recently Quenzel and Kaestner (1980), have also reported intensities for models of the ocean–atmosphere system, where the lower boundary of the atmosphere is a rough ocean surface. Raschke's computations are based on a simple model of the atmosphere, whereas Plass *et al.* and Quenzel and Kaestner have considered more realistic model atmospheres. However, except for Fraser and Walker, Dave, and Kattawar *et al.*, all other authors have neglected the polarization of the diffuse radiation in the atmosphere as well as the polarization of the reflected radiation (from the rough ocean surface) in their computations.

In this paper, we present the details of a radiative transfer scheme, which is applicable to realistic ocean–atmosphere systems and takes into consideration all orders of scattering, as well as polarization. However, the present version of surface reflection neglects the effect of wind direction, shadowing, multiple reflections, and the scattering of light from below the ocean surface. In this paper, we also give a comparison of our results with those of Fraser and Walker, and Dave for a Rayleigh atmosphere with an optically smooth lower boundary, with Mullamaa

0022-4928/82/030656-10$06.50

(1964) for a rough ocean with no atmosphere, and with Plass *et al.* for a model closely approximating the real ocean–atmosphere system. In this paper we also present a detailed study of intensity and degree of polarization in different models of the ocean–atmosphere system. The organization of this paper is as follows: we give the theoretical background and the computational procedure of the numerical scheme in Section 2 and the results of the comparison in Section 3. The details of the reflection law from the ocean surface are given in Appendix A.

2. Theoretical background

a. General

Numerical schemes to compute the radiances in an ocean–atmosphere system can be developed in many ways. Plass *et al.* (1975) have utilized the Monte Carlo technique, whereas Raschke (1972) has followed the conventional method of expanding the phase function in a Fourier series and utilized an iterative scheme to solve the radiative transfer equation for the ocean–atmosphere system. Another possible method of developing a numerical scheme is to compute the reflection and transmission matrices of the atmosphere and the ocean separately, and then treat the whole system—in two-slab approximations. This method, although sound in principle, is not very practical in its general form. One of the reasons is related to the homogeneity of the atmosphere. If the atmosphere is homogeneous, then the reflection and transmission matrices for light entering the atmosphere from the top at an angle θ_i would be the same as light entering the atmosphere from the bottom at the same angle. However, if the atmosphere is inhomogeneous vertically, then we would require two sets of reflection and transmission matrices—one for light entering the atmosphere from the top while the other for the light entering the atmosphere from the bottom. Since computation of reflection and transmission matrices, even for one angle of incidence, is very time consuming, we describe in the following sections another scheme which is based on a modified version of the two-slab approximation. In this scheme, we divide the atmosphere into layers of equal optical thicknesses and solve the radiative transfer equation iteratively while reflecting the radiation leaving the base of the atmosphere back into the atmosphere using the reflection matrix for the rough ocean. In subsection b) we give some of the necessary expressions and in subsection c), the details of the reflection matrix for the rough ocean are described.

b. Equation of radiative transfer

The equation of radiative transfer through a nonemiting, plane-parallel and horizontally homogeneous atmosphere is generally written as (Chandrasekhar, 1950)

$$\frac{\mu d\mathbf{I}(\tau;\mu,\phi)}{d\tau} = \mathbf{I}(\tau;\mu,\phi) - \mathbf{J}(\tau;\mu,\phi), \qquad (1)$$

where

$$\mathbf{J}(\tau;\mu,\phi) = \frac{\omega_0}{4\pi}\left[\int_{\omega'} \mathbf{P}(\tau;\mu,\phi;\mu',\phi')\mathbf{I}(\tau;\mu',\phi')d\omega' + \mathbf{P}(\tau;\mu,\phi;-\mu_0,\phi_0)\pi\mathbf{F}_0(-\mu_0,\phi_0)e^{-\tau/\mu_0}\right]. \qquad (2)$$

In Eqs. (1) and (2), τ is the optical depth measured from the top of the atmosphere to τ_b at its base, μ is the absolute value of the cosine of the scattering angle measured with respect to the local zenith, ϕ is the azimuth direction and the differential $d\omega' = d\mu' d\phi'$. $\mathbf{I}$ is the columnar vector of the four Stokes parameters for the light at level τ, and $\mathbf{J}$ is the scattering source matrix which represents virtual emission in a cone of unit solid angle in the direction (μ, ϕ). $(4\pi)^{-1}\mathbf{P}$ is the phase matrix relating the scattering contribution to the beam traveling in the direction (μ, ϕ) from the incident light in the direction (μ', ϕ') and $\pi\mathbf{F}_0$ is the columnar vector of the four Stokes parameters of the parallel flux in the direction $(-\mu_0, \phi_0)$ incident at the top of the atmosphere.

For a planetary atmosphere, the boundary conditions are generally written as

$$\mathbf{I}(0;-\mu,\phi) = 0, \qquad (3)$$

$$\mathbf{I}(\tau_b;+\mu,\phi) = 0. \qquad (4)$$

These boundary conditions imply that no diffuse radiation enters the planetary atmosphere either from the top or the base of the atmosphere.

To compute the four Stokes parameters in an ocean–atmosphere system, we simply modify the boundary condition (4) as

$$\mathbf{I}(\tau_b;+\mu,\phi)d\omega = \left[\int \mathbf{f}(+\mu,\phi;-\mu',\phi';x)\mathbf{I}(\tau_b;-\mu',\phi')d\omega' + \mathbf{f}(+\mu,\phi;-\mu_0,\phi_0;x)\pi\mathbf{F}_0 e^{-\tau_b/\mu_0}\right], \qquad (5)$$

where $\mathbf{f}(+\mu, \phi; -\mu', \phi'; x)$ represents the reflection law of the rough ocean. The parameter x in the argument of the reflection law represents all physical parameters (in addition to μ, ϕ, μ' and ϕ') necessary to describe the law. Note that in writing the boundary condition (5), we have neglected the terms describing (a) the contribution from the multiple reflections between elements of the sea surface and (b) the effect of shadowing. In Appendix A, we show that the reflection law for the rough ocean can be written as

$$\mathbf{f}(+\mu,\phi;-\mu',\phi';x) = \frac{\mu_\chi}{\mu\mu_n} P(Z_x, Z_y)dZ_x dZ_y \mathbf{L}(\pi - i_2)\mathbf{R}(\chi)\mathbf{L}(-i_1), \qquad (6)$$

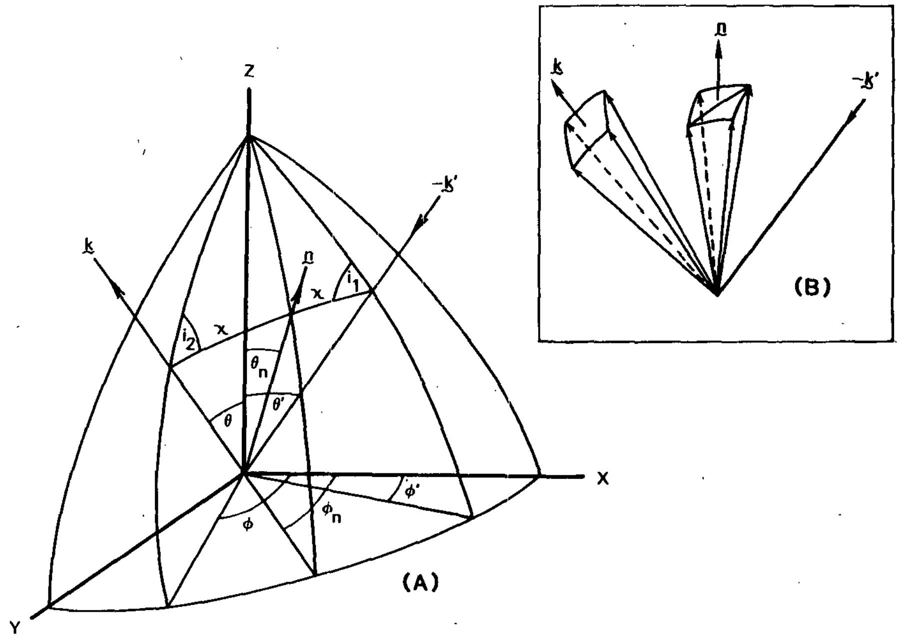

FIG. 1. (A) Geometrical relationship between a pencil of radiation incident in the direction ($-\mathbf{k}'$), the reflected radiation in the direction ($\mathbf{k}$) and the normal ($\mathbf{n}$) to the reflecting facet. (B) shows that as long as the normal lies within the cone of the normal, the reflected ray remains within the cone of reflection.

where $\mathbf{L}(-i_1)$ is the rotation matrix which rotates the Stokes parameters of the radiation, incident in the direction $(-\mu', \phi')$ from the vertical plane to the scattering plane, and $\mathbf{L}(\pi - i_2)$ is the rotation matrix which rotates the Stokes parameters of the radiation (after scattering) from the scattering plane to the vertical plane. The scattering plane contains the incident beam, the normal to a reflecting facet, and the beam reflected from it. i_1 is the angle between the scattering plane and the vertical plane containing the incident beam, and i_2 is the angle between the scattering plane and the vertical plane containing the scattered beam; i_1 and i_2 are functions of the incident and reflected directions (see Fig. 1). Chandrasekhar (1950) gives expressions for $\mathbf{L}(-i_1)$ and $\mathbf{L}(\pi - i_2)$. $\mathbf{R}(\chi)$ is the Fresnel reflection matrix relating the incident and reflected intensity matrices in the scattering plane; χ is the angle between the incident beam and the normal in the scattering plane and $\mu_\chi = \cos\chi$. $P(Z_x, Z_y)$ is the slope probability distribution of the small facets on the ocean surface, and dZ_x and dZ_y are the infinitesimal changes in the slope components in the X- and Y-directions; μ_n is the cosine of the normal to the reflecting facet measured with respect to the local zenith. The explicit expression for the slope probability function $P(Z_x, Z_y)$ and the reflection matrix $\mathbf{R}(\chi)$ are given in Cox and Munk (1954, 1955) and Dave (1972).

To compute the four Stokes parameters of the diffuse radiation in a model of the ocean–atmosphere system, we solve the radiative transfer equation (1) with boundary conditions (3) and (5). We follow the Herman and Browning (1965) numerical scheme to obtain solutions. The scheme is based on the Gauss-Seidel iterative technique. In this scheme, the model atmosphere is divided into plane-parallel layers and the radiative transfer equation is solved by numerically integrating the source matrix over the optical depth τ, the polar angle θ and the azimuth angle ϕ.

Since the scheme utilizes an iterative technique, the implementation of the boundary condition (5), i.e., introduction of the rough ocean surface at the base of the atmosphere, is simple. For a given model of the atmosphere we first compute the direct and downward diffuse radiation leaving the base of the atmosphere and then use the previously computed reflection matrix of the ocean and reflect both the direct and the diffuse radiation back into the atmosphere. In our present scheme we assume that all the radiation transmitted into the ocean is absorbed completely. In the next section we give the details of the numerical computations of the reflection matrix and then proceed with the discussion of the diffuse radiation in the model atmosphere.

c. *Reflection matrix of the rough ocean*

The reflected radiation just above the ocean surface consists of two parts: one due to reduced parallel flux and the other due to the downward diffuse radiation leaving the base of the atmosphere. In almost all cases, the first term dominates over the second. To compute the four Stokes parameters of the reflected radiation, we assume that parallel rays incident at an angle (μ', ϕ') are reflected in the direction (μ, ϕ) confined in a cone of solid angle Ω. From the elementary consideration of the reflection, it is obvious that the intensity over the cone will vary according to the slope distribution on the ocean surface. To compute the four Stokes parameters at each point over the cone, we divide the cone into small meshes of angular dimension $\Delta\theta$ and $\Delta\phi$ and determine the normal to the facet that would reflect the incident beam to the center of the small mesh (say μ, ϕ). Since the incident beam, the normal, and the reflected beam all lie in the same plane, we can easily determine the angles χ, i_1, i_2, θ_n and ϕ_n numerically from the following relations of the spherical trigonometry (see Fig. 1 for the definitions of these angles)

$$\cos 2\chi = \mu'\mu + [(1-\mu'^2)(1-\mu^2)]^{1/2}\cos(\phi'-\phi), \quad (7)$$

$$\sin i_1 = \frac{\sin(\phi'-\phi)}{\sin 2\chi}(1-\mu^2)^{1/2}, \quad (8)$$

$$\sin i_2 = \frac{\sin(\phi'-\phi)}{\sin 2\chi}(1-\mu'^2)^{1/2}, \quad (9)$$

$$\mu_n = \mu'\mu_\chi + [(1-\mu_\chi^2)(1-\mu'^2)]^{1/2}\cos i_1\,, \quad (10)$$

$$\sin(\phi'-\phi_n) = \sin i_1[(1-\mu_\chi^2)(1-\mu_n^2)^{-1}]^{1/2}, \quad (11)$$

where

$$\mu_n = \cos\theta_n \quad \text{and} \quad \mu_\chi = \cos\chi. \quad (12)$$

Once we determine the angles (i.e., χ, i_1, i_2, θ_n, ϕ_n), the computations of the slope distribution $P(Z_x, Z_y)$ and the matrix elements of $\mathbf{L}(-i_2)$, $\mathbf{L}(-i_1)$ and $\mathbf{R}(\chi)$ are straightforward. The only other quantity in Eq. (6) that remains to be computed is dZ_xdZ_y. It can be computed in several ways. In Appendix A we show that it is related to a normal $\mathbf{n}$ of surface element, which reflects the light incident in the direction $-\mathbf{k}'$, confined in a solid angle $d\omega'$, into a solid angle $d\omega$ in the direction $\mathbf{k}$. We compute dZ_xdZ_y numerically. We assume that parallel rays incident on the rough ocean surface are reflected in a cone of angular dimension $\Delta\theta$ and $\Delta\phi$. We determine four normals to the facets that would reflect light to the four corners of the ($\Delta\theta$, $\Delta\phi$) mesh (see Fig. 1b). Using the four normals we construct two spherical triangles on a unit sphere. The area of the two triangles gives the solid angle $\Delta\omega_n(=\Delta\mu_n\Delta\phi_n)$ which is related to $\Delta Z_x\Delta Z_y$ by Eq. (A6b) of Appendix A. From geometric optics, it is obvious that as long as the normal lies within the solid angle $\Delta\omega_n$ in the direction ($\mu_n\phi_n$), the reflected ray is confined in the solid angle $\Delta\omega$ in the direction (μ, ϕ).

To compute the reflection matrix of the rough ocean for the ocean–atmosphere model, we assume with Cox and Munk (1955) that the variance of the slopes of the waves on the ocean surface is linearly related to the wind speed over the ocean surface. This assumption reduces the computation time considerably, because it makes the reflection matrix independent of the azimuth direction (ϕ') of the incident light. The computations of the reflection matrix consist of determining the average value of the matrix elements for light reflected in the direction ($+\mu_m$, ϕ_n) for a mesh of angular dimension ($\Delta\mu_m$, $\Delta\phi_n$) when the light is incident from all directions and repeating the calculations for different values of m and n. Note that these meshes correspond to the integration meshes used for integrating the radiative transfer equation.

3. Results

In the following subsections we present some results (obtained by utilizing our code) on the intensity and degree of polarization of diffuse radiation for various models of the ocean–atmosphere system. Also, wherever possible, we compare our results with those obtained by others for identical or almost identical models. Our motive for comparing the results is to establish the relative precision of different computations. In all of our calculations, the strength of the incident parallel solar flux is π.

a. Direct sunlight reflected by a rough ocean

In this subsection we compare our results with those of Mullamaa (1964) for the intensity and degree of polarization of the light reflected from a rough ocean surface. No atmosphere is present in this comparison. For a solar zenith angle of 58.7° we show in Fig. 2 a comparison of the intensity just above the ocean surface for wind speeds of 2, 5, and 15 m s^{-1}. In both our and Mullamma's computations, the slope distribution is a binormal distribution in which the variances of the slopes depend on the wind direction, as specified by Cox and Munk (1954). The wind vector is parallel to the principal plane, which contains the zenith and sun-line directions. The wind blows from right to left relative to the abscissa of Fig. 2. As is obvious from Fig. 2, the agreement between the two computations is excellent. A comparison of numerical values, which we do not give in this paper, shows that the two computations agree up to three significant figures. For the same value of the solar zenith angle we also show, in Fig. 3, a comparison of the degree of polarization. The reflected light is highly polarized, and the degree of polarization is independent of wind velocity. The reason is that both computations neglect the effect of white caps, and in the absence of white caps the degree of polarization of the reflected light depends not on the intensity of polarized light, but only on

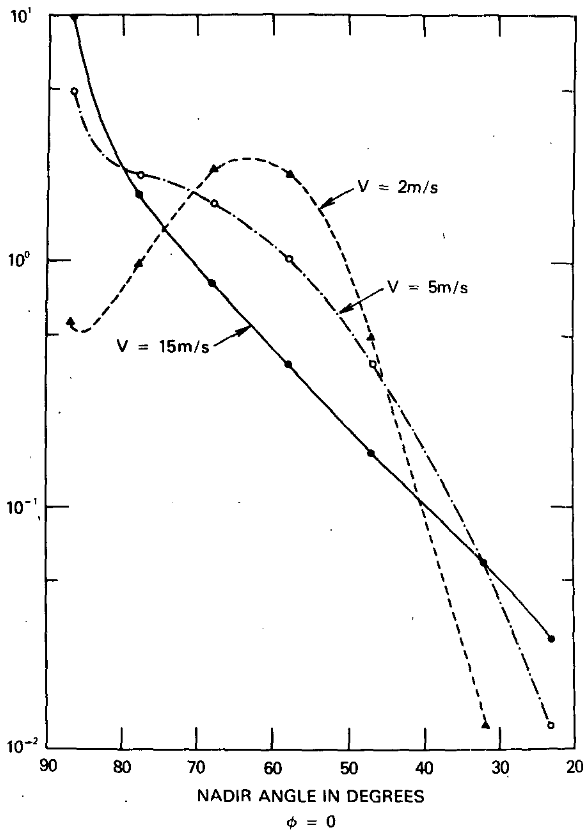

FIG. 2. A comparison of intensities of direct sunlight reflected from a rough sea surface in the principal plane. The normals to the sea surface slopes are given by the Cox-Munk (1954) distribution function that depends on wind direction. The solar zenith angle $\theta_0 = 58.7°$. The lines give our computed values, whereas the symbols give Mullamaa's (1964) values.

the slope of a surface facet required to reflect the incident beam in the direction of observation.

b. Rayleigh atmosphere and smooth ocean

We have mentioned earlier that Fraser and Walker (1968) first reported the intensity and the degree of polarization of diffuse radiation for a Rayleigh atmosphere resting on an optically-smooth ocean surface. Later, Dave (1972) and Kattawar *et al.* (1973) also developed radiative transfer codes for computing the intensity and the degree of polarization of diffuse radiation for a realistic model atmosphere resting on our optically-smooth ocean surface. For the purpose of comparison, we have computed the intensity and degree of polarization for a standard (molecular) atmosphere ($\tau = 0.15$, $\theta_0 = 60°$) resting on a smooth ocean ($m = 1.3417 - 0.0i$) by utilizing our code and those of Dave, and Fraser and Walker. The computations show that at the top of the atmosphere the absolute difference between our intensity value and others is <0.7%. Similarly, the absolute difference in the degree of polarization is <0.005. We find similar results hold between the three computations at the base of the atmosphere.

c. Atmosphere with haze and rough ocean

1) THE MODEL ATMOSPHERE

To compute the intensity and degree of polarization of the diffuse radiation for a realistic model of the ocean–atmosphere system, we assume that our model atmosphere consists of the standard gas, particulates and the trace gases (for example, ozone). The model is inhomogeneous and finite in the vertical direction, homogeneous and infinite in the horizontal direction and is separated at the lower boundary by a rough ocean surface. In the model atmosphere, the standard gas, particulates and ozone are distributed vertically according to Elterman's (1964) distributions; and their optical thicknesses for a wavelength of $\lambda = 0.7\mu$ are respectively, 0.037, 0.214, and 0.008. Also, the particulates are non-absorbing (refractive index $m = 1.5 - 0.0i$) and their size distribution follows a Junge distribution with a slope of −4, i.e.,

$$\frac{dn}{dr} = C, \qquad \text{for} \quad 0.03 \leqslant r \leqslant 0.1\ \mu,$$

$$\frac{dn}{dr} = C\left(\frac{0.1}{r}\right)^4, \quad \text{for} \quad 0.1 \leqslant r \leqslant 5.0\ \mu.$$

For the rough ocean surface, we assume that the slope distribution of the waves is independent of wind direction. Also, as we stated earlier, we neglect the effect of shadowing and multiple reflection on the surface, and assume that all the radiation that is transmitted through the ocean surface is absorbed completely.

2) DIFFUSE INTENSITY

In this subsection, we first compare our results with those of Plass *et al.* (1975), who, utilizing the Monte Carlo technique, have reported on the intensity of diffuse radiation for an almost identical model

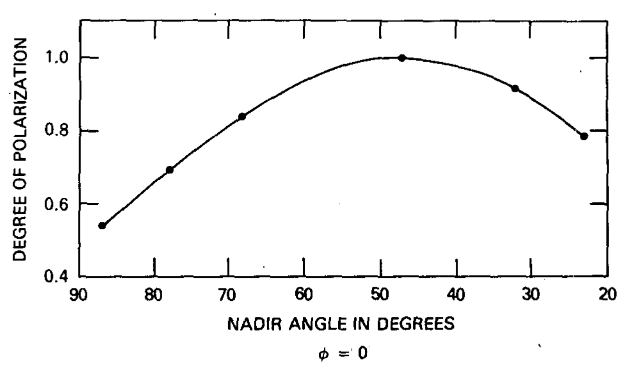

FIG. 3. A comparison of the degree of polarization of the light reflected by a rough sea surface. The conditions of Fig. 2 apply.

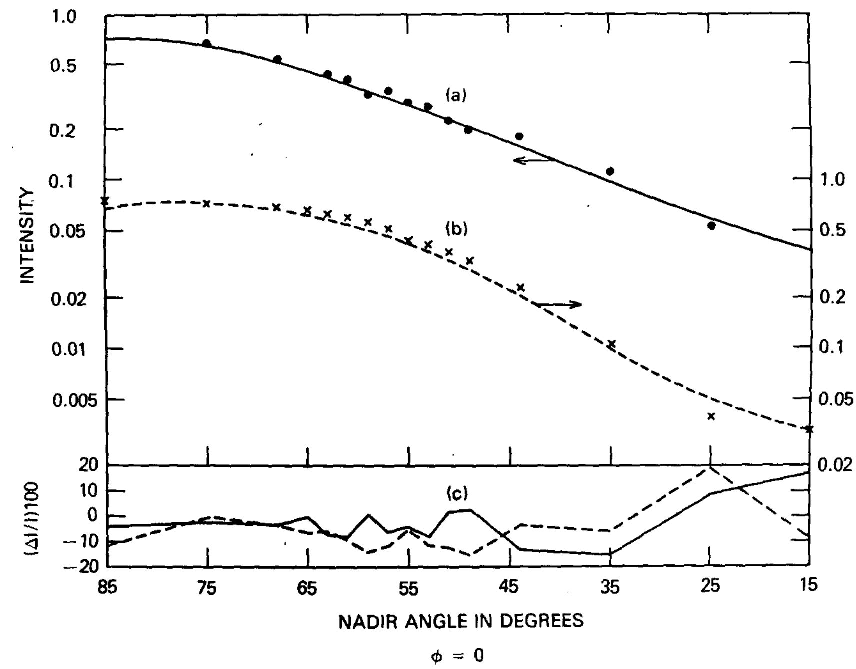

FIG. 4. A comparison of intensities of light leaving the top of the atmosphere. The solid (a) and dashed (b) lines give our results for wind speed of 10.3 and 5.15 m s^{-1}, respectively. The symbols give the values computed by Plass *et al.* (1975). (c) The relative value of our intensities minus those of Plass *et al.*

of the ocean–atmosphere system described in the preceding section. Then, we show our results on the intensity of diffuse radiation for wind speeds of 5.15 and 10.3 m s^{-1} and solar zenith angles of 20 and 57°.

(i) Comparison with Plass *et al.* Figs. 4a and 4b show the intensity of upwelling diffuse radiation at the top of the atmosphere obtained by utilizing our code and that of Plass *et al.* The solar zenith angle for the two figures is 57°, and the wind speeds are respectively 10.3 (Fig. 4a) and 5.15 m s^{-1} (Fig. 4b). For the purpose of comparison, we have normalized Plass *et al.*'s intensities to π units of incident parallel flux at the top of the atmosphere. Both Figs. 4a and 4b show good qualitative agreement; however, there is a bias in the two computations. Plass *et al.*'s intensities for $35 \leqslant \theta \leqslant 65°$ are generally higher than ours. We show the bias expressed in percentage in Fig. 4c. It is more pronounced at 5.15 m s^{-1} than at 10.3 m s^{-1}. For a wind speed of 5.15 m s^{-1} we also compare the upwelling intensities just above the ocean surface (Fig. 5). We find that for the range of nadir angles $37° \leqslant \theta \leqslant 68°$, the bias is $\sim$17%. As discussed earlier in Section 3a, our computed intensities of sunlight reflected from the sea and Mullamaa's intensities agree to three significant figures. We cannot account for the discrepancy between our results and those of Plass *et al.*

(ii) Diffuse intensity as a function of wind speed and solar zenith angle. Figs. 6a and 6b depict the intensity of the radiant energy leaving the top of the model atmosphere in the principal plane as a function of the nadir angle. The solar zenith angle is 20° for (a) and 57° for (b). For small solar angle [Fig. 6a], the maximum intensity of the glint decreases with

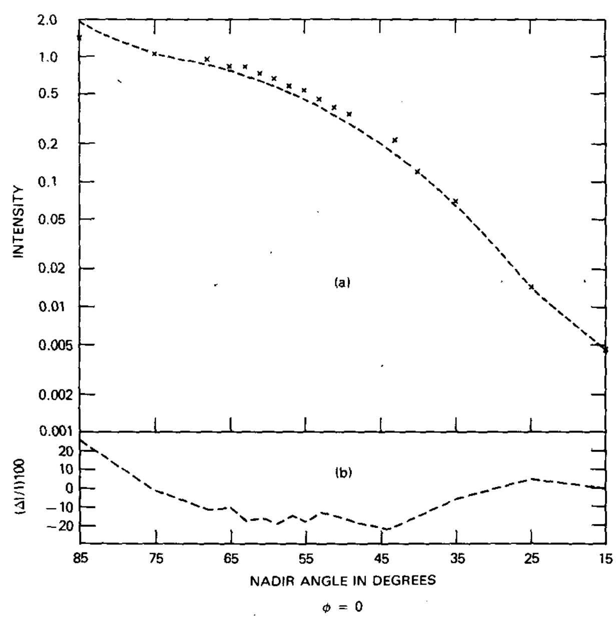

FIG. 5. (a) A comparison of our intensity (dashed curve) and that of Plass, *et al.* (1975) (symbols). (b) The relative difference between the intensities.

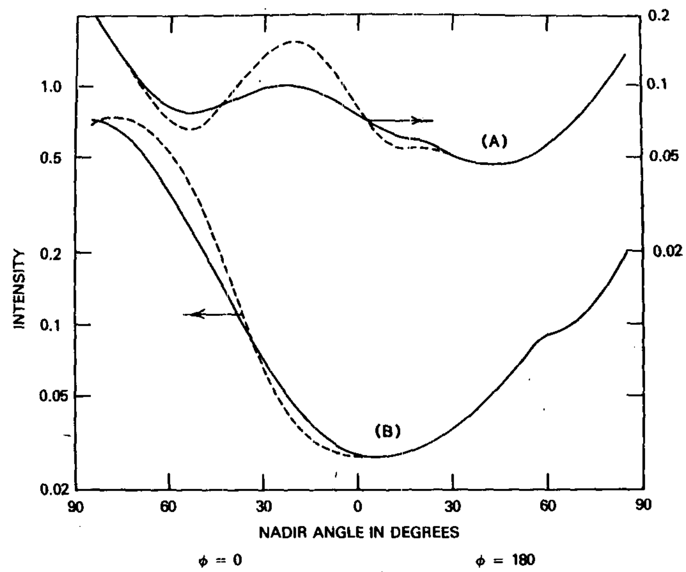

FIG. 6. The intensity of light emerging in the principal plane from the top of a model atmosphere with aerosols. The slope normals to the rough ocean are given by a Cox-Munk distribution function. The solar zenith angle (θ_0) is 20° in (A) and 57° in (B). The surface wind speeds are 5.15 and 10.3 m s^{-1} for the dashed and continuous lines, respectively.

increasing wind speed. Although the glint pattern broadens with increasing wind speed, the half-width of the pattern is difficult to specify at the higher wind speed and has not changed much from that of the lower wind speed. For a larger solar zenith angle (Fig. 6b) the intensity changes monotonically for θ near θ_0, and the glint is not apparent. When we examine the intensity as a function of the azimuth angle for $\theta = \theta_0$, we find that the glint is narrower for low sun (57°) than it is for high sun (20°). The full widths at half maximum are, respectively, 48 and 60°.

We have also examined (in the principal plane) the intensity of the reflected radiation just above the ocean surface. As expected, the general features are the same as in Figs. 6a and b, except that at the base of the atmosphere, the maximum intensity is slightly lower than at the top of the atmosphere and the minimum intensity decreases by an order of magnitude.

3) DEGREE OF POLARIZATION

We show the degree of polarization of the upwelling diffuse radiation at the ocean surface in Fig. 7 and at the top of the atmosphere in Fig. 8. The solar zenith angle is 20°. The degree of polarization at the surface is maximum near the Brewster angle on both sides of the nadir, irrespective of the solar zenith angle. The degree of polarization depends slightly on wind speed, contrary to the data (Fig. 3), where no skylight is present. Skylight is polarized, and different proportions are reflected in a given direction, depending on wind speed. White caps are

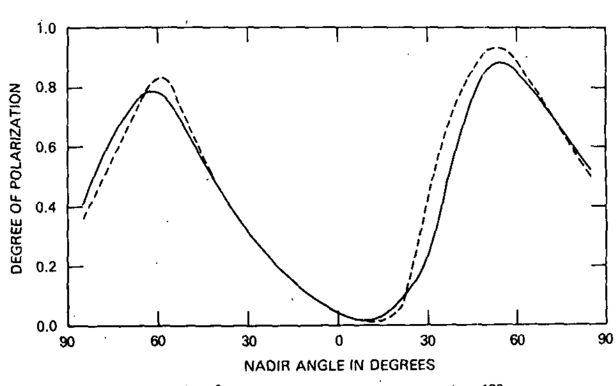

FIG. 7. The degree of polarization just above a sea surface of light reflected from it. The solar zenith angle θ_0 = 20°. The dash and continuous lines apply when the wind speed are 5.15 and 10.3 m s^{-1}, respectively.

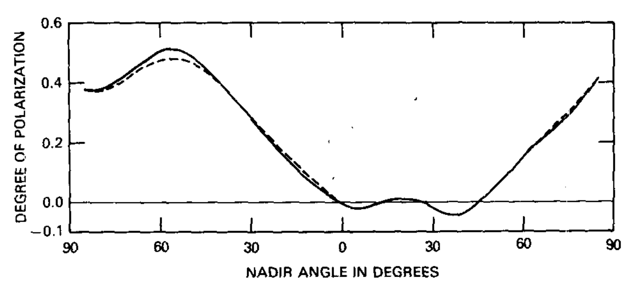

FIG. 8. The degree of polarization of light emerging from the top of the atmosphere for the same conditions used in Fig. 7.

neglected, and they would decrease the absolute value of the degree of polarization.

At the top of the atmosphere (Fig. 8), however, the high degree of polarization persists in the $\phi = 0°$ plane, but it is greatly reduced in the $\phi = 180°$ plane. This interesting behavior can be easily explained as follows: at the top of the atmosphere, in the $\phi = 180°$ plane, the highly polarized light reflected from the surface near the Brewster angle constitutes a very small fraction of the total radiation, while the airlight, which is weakly polarized, dominates. Hence, the degree of polarization of the total radiation is small. On the other hand, in the $\phi = 0°$ plane, the highly polarized light from the surface near the Brewster angle is comparable in intensity to that of the airlight, which is moderately polarized also, and, therefore, at the top of the atmosphere, the high degree of polarization near the Brewster angle persists.

4) EFFECT OF REPLACING THE OCEAN SURFACE BY A LAMBERTIAN SURFACE

In Figs. 9 and 10 we show the intensity and degree of polarization of the upwelling diffuse radiation at the top of the atmosphere for two models that we constructed from the models of the preceding section by replacing the rough ocean by (a) a surface which absorbs all the radiation that falls on it and (b) a Lambertian surface which reflects the same amount of energy as the rough ocean (6.9%). The results of the former are shown by a dashed line, while the results of the latter are shown by a dash-dot line. For completeness, we also show by a solid line the results for a model atmosphere with a rough ocean

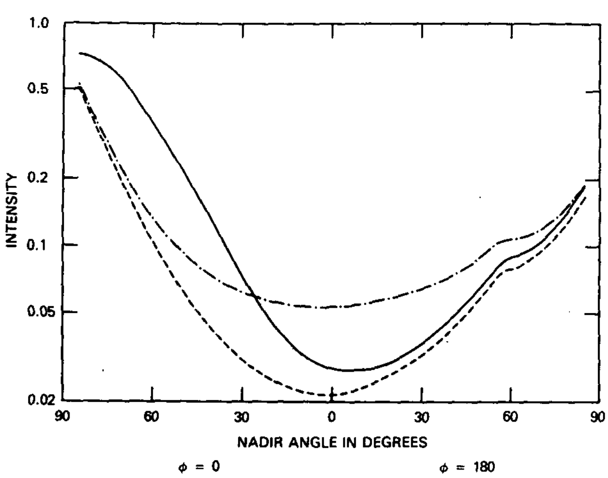

FIG. 9. Comparisons of intensities of light emerging from the top of a model atmosphere with three types of surface reflectance. The dash, continuous, and dash-dot lines apply, respectively, to a surface with zero reflectance, a rough surface where the wind speed is 10.3 m s^{-1} and the reflectance is 0.069, and a Lambert surface with the same reflectance $\theta_0 = 57°$.

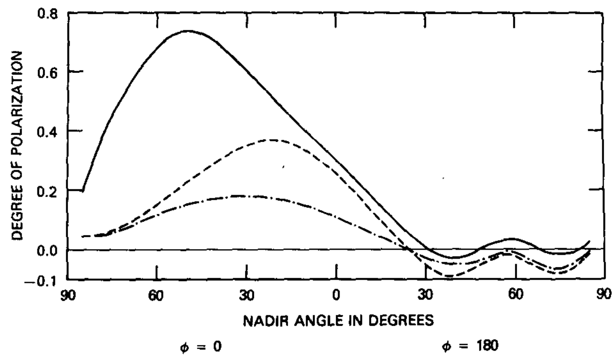

FIG. 10. A comparison of the degree of polarization for the conditions of Fig. 9.

surface (V = 10.3 m s^{-1}). The solar zenith angle is 57° for all three models. Without surface reflection, the intensity is asymmetrical with respect to the nadir because of the relative strong forward-scattering by the aerosols. The asymmetry is reduced with Lambert surface reflection. The strongly anisotropic nature of the surface reflection of a rough sea surface, however, causes strong asymmetry in this model with a small optical thickness ($\tau = 0.259$).

The degree of polarization of the light emerging from the top of the atmosphere in the principal plane is given in Fig. 10. Without surface reflection, the maximum degree of polarization is only 0.37, since most of the light is scattered by the aerosols; and the light scattered from them is weakly polarized. The light reflected from the surface with Lambert reflection is unpolarized and reduces the absolute value of the polarization. The rough-surface reflection has a strong effect on the degree of polarization. The bright glint near 57° is strongly polarized (the Brewster angle is 53°). The weak, but highly polarized, reflection toward the anti-solar direction (in the plane $\phi = 180°$) causes four neutral points to appear, rather than only one neutral point which appears with the other two models.

4. Summary

In this paper we have described a radiative transfer scheme that enables us to compute the four Stokes' parameters and, from them, the intensity and degree of polarization of the light leaving the top, base, and any level of the atmosphere in an ocean–atmosphere system. To establish the reliability of the numerical scheme and the computer code, we have compared the results obtained by our code and others for different models. The intensity and degree of polarization of sunlight reflected from a rough ocean surface in the absence of an atmosphere is compared with Mullamaa's data. The two sets of data agree to three significant figures.

Our computations are compared with those of Dave (1972) and Fraser and Walker (1968) for a model with a Rayleigh atmosphere and a smooth surface. The intensities agree within 0.7%. The maximum absolute discrepancy in the degree of polarization is 0.005. For a more realistic ocean–atmosphere model, there is good qualitative agreement between our intensities and those computed by Plass *et al.* (1975), who utilize the Monte Carlo technique.

These comparisons indicate that in our ocean–atmosphere computations, the reflective laws at the lower boundary have been properly taken into account and that our numerical scheme is reliable and can be used to investigate the intensities and degree of polarization of diffuse radiation leaving the top of the atmosphere in an ocean–atmosphere system.

In addition to the comparisons, we have also investigated the change in intensity and degree of polarization at the top of the atmosphere, when the rough ocean surface is replaced by a Lambertian surface that reflects the same amount of energy in the atmosphere as the rough ocean. These results clearly indicate that for a thin atmosphere, we would arrive at erroneous conclusions if we attempted to explain the earth-orbiting-satellite data in the context of a Lambertian surface.

APPENDIX

Reflection by a Rough Surface

Dave (1972) has given the explicit expressions for the elements of the reflection matrix for a smooth surface. In this appendix we give the expressions for the Stokes parameters of light reflected by a rough surface.

Let us assume that a pencil of radiation in the direction $(-\mathbf{k}')$ and confined in a small solid angle $\Delta\omega'$ falls on a surface that consists of a large number of small facets. Let us also assume that the normals $(\mathbf{n})$ to the facets are randomly oriented in space and follow a distribution function $P(\mathbf{n})$. If $\mathbf{I}(-\mathbf{k}')$ refers to the intensity matrix of the four Stokes parameters of the incident beam, then the total flux $\Delta\mathbf{F}$ falling on all the illuminated facets, which reflect the incident beam into a cone of solid angle $\Delta\omega$ in the direction $\mathbf{k}$, can be written as

$$\Delta\mathbf{F} = \sum_j \mathbf{I}(-\mathbf{k}')\Delta\omega'|\mathbf{n}_j\cdot\mathbf{k}'|\Delta S_j P(\mathbf{n}_j)\Delta\omega_n\,, \quad \text{(A1)}$$

where ΔS_j is the actual area of the jth facet, $\mathbf{n}_j$ is the unit vector in the direction of the normal to the jth facet and $P(\mathbf{n}_j)$ represents the probability that the normal $\mathbf{n}$ to the facet occurs within the solid angle $\Delta\omega_n(\Delta\omega_n = \Delta\mu_n\Delta\phi_n)$. The summation is over the subsets of facets whose normals lie within $\Delta\omega_n$. If ΔA_j represents the projected area of ΔS_j on a horizontal surface [i.e., $\Delta S_j = \Delta A_j(\mathbf{z}\cdot\mathbf{n}_j)$] then from Eq. A1 we can write

$$\Delta\mathbf{F} = \mathbf{I}(-\mathbf{k}')\Delta\omega' P(\mathbf{n})\Delta\omega_n \frac{\Delta A}{(\mathbf{z}\cdot\mathbf{n})}|\mathbf{n}\cdot\mathbf{k}'|, \quad \text{(A2)}$$

where $\mathbf{z}$ is a unit vector along the local vertical, and $\Delta A = \Sigma_j\Delta A_j$ is the total area projected on a horizontal plane of those facets whose normals lie within $\Delta\omega_n$.

Note that in Eqs. (A1) and (A2), we have defined the Stokes parameters of the incident beam in a vertical plane with respect to the unit vectors $\mathbf{l}$ and $\mathbf{r}$, where $\mathbf{k}' = \mathbf{l}\times\mathbf{r}$, and $\mathbf{r}$ is orthogonal to the plane containing the incident beam. This vertical plane contains the unit vectors $-\mathbf{k}'$ and $\mathbf{z}$. To refer the Stokes parameters of the incident beam in the scattering plane, we multiply (A2) by $\mathbf{L}(-i_1)$ where i_1 is the angle between the vertical plane and the scattering plane. [The explicit form of the rotation matrix $\mathbf{L}(-i_1)$ is given in Chandrasekhar (1950).]

If we assume that the light from each facet is reflected according to Fresnel's law, then the Stokes parameters for the light reflected into the cone $\Delta\omega$ (in the direction $\mathbf{k}$, i.e., $\mathbf{I}(\mathbf{k})$ can be written as:

$$\mathbf{I}(\mathbf{k})\Delta\omega\Delta A(\mathbf{z}\cdot\mathbf{k}) = \mathbf{L}(\pi - i_2)\mathbf{R}(\mathbf{n}\cdot\mathbf{k}'; m) \times \mathbf{L}(-i_1)I(-\mathbf{k}')\Delta\omega' P(\mathbf{n})\Delta\omega_n|\mathbf{n}\cdot\mathbf{k}'|\frac{\Delta A}{(\mathbf{z}\cdot\mathbf{n})}, \quad \text{(A3)}$$

where $\mathbf{R}(\mathbf{n}, \mathbf{k}'; m)$ is the Fresnel reflection matrix. It is function of both the angle of incidence and the index of refraction m of the surface. It should be noted that in Eq. A3, we have rotated the Stokes parameters of the reflected beam from the scattering plane to the vertical plane, which contains both the reflected beam in the direction $\mathbf{k}$ and the local vertical $\mathbf{z}$. To refer them to the vertical plane, we have used the matrix $\mathbf{L}(\pi - i_2)$ where i_2 is the angle between the planes defined by $(\mathbf{k}, \mathbf{n})$ and $(\mathbf{k}, \mathbf{z})$.

If we define

$$\mu' = |\mathbf{z}\cdot\mathbf{k}'|, \qquad \mathbf{I}(\mu', \phi') = \mathbf{I}(-\mathbf{k}'),$$
$$\mu = |\mathbf{z}\cdot\mathbf{k}|, \qquad \mathbf{I}(\mu, \phi) = \mathbf{I}(\mathbf{k}),$$
$$\mu_n = \mathbf{z}\cdot\mathbf{n}, \qquad P(\mu_n, \phi_n) = P(\mathbf{n}),$$
$$\mu_\chi = \mathbf{n}\cdot\mathbf{k}', \qquad \mathbf{R}(\chi) = \mathbf{R}(\mathbf{n}, \mathbf{k}'; m),$$

then Eq. A3 becomes

$$\mathbf{I}(\mu, \phi) = \frac{\mu_\chi}{\mu\mu_n}P(\mu_n, \phi_n)\Delta\omega_n\mathbf{L}(\pi - i_2) \times \mathbf{R}(\chi)\mathbf{L}(-i_1)\mathbf{I}(\mu', \phi')\frac{\Delta\omega'}{\Delta\omega}. \quad \text{(A4)}$$

Note that the functional notation for $\mathbf{R}$ is simplified by omitting m, which is constant for the models used here. In many problems, it is more convenient to express the probability distribution function $P(\mu_n, \phi_n)$ in terms of the x and y components of the slope of the facet z. To express $P(\mu_n, \phi_n)$ as $P(z_x, z_y)$, we find that the slope components x and y are related to $\theta_n = (\cos^{-1}\mu_n)$ and ϕ_n as

$$Z_x = \tan\theta_n \cos\phi_n , \quad \text{(A5a)}$$

$$Z_y = \tan\theta_n \sin\phi_n , \quad \text{(A5b)}$$

$$\Delta Z_x \Delta Z_y = \left. \begin{vmatrix} \dfrac{\partial Z_x}{\partial\theta_n} & \dfrac{\partial Z_x}{\partial\phi_n} \\ \dfrac{\partial Z_y}{\partial\theta_n} & \dfrac{\partial Z_y}{\partial\phi_n} \end{vmatrix} \right\} , \quad \text{(A6a)}$$

$$\Delta Z_x \Delta Z_y = \sec^3\theta_n \Delta\omega_n = \frac{\Delta\omega_n}{\mu_n{}^3} . \quad \text{(A6b)}$$

With this transformation, Eq. (A4) becomes

$$\mathbf{I}(\mu, \phi) = \frac{\mu_\chi}{\mu\mu_n} P(\mu_n, \phi_n)\mu_n{}^3(\Delta Z_x \Delta Z_y)\mathbf{L}(\pi - i_2) \times \mathbf{R}(\chi)\mathbf{L}(-i_1)\mathbf{I}(\mu', \phi') \frac{\Delta\omega'}{\Delta\omega} . \quad \text{(A7)}$$

If we define

$$P(Z_x, Z_y) = \mu_n{}^3 P(\mu_n, \phi_n), \quad \text{(A8)}$$

then

$$\mathbf{I}(\mu, \phi) = \frac{\mu_\chi}{\mu\mu_n} P(Z_x, Z_y)\Delta Z_x \Delta Z_y \mathbf{L}(\pi - i_2) \times \mathbf{R}(\chi)\mathbf{L}(-i_1)\mathbf{I}(\mu', \phi') \frac{\Delta\omega'}{\Delta\omega} . \quad \text{(A9)}$$

Cox and Munk (1954) give two distributions: one in which the wave slopes are independent of wind direction; then the slopes Z_x and Z_y are independent with the same variance; in the second distribution, the slopes depend on the wind direction.

REFERENCES

Chandrasekhar, S., 1950: *Radiative Transfer.* Oxford University Press, 393 pp.

Cox, C., and W. H. Munk, 1954: The measurement of the roughness of the sea surface from photographs of the sun glitter. *J. Opt. Soc. Amer.*, **44,** 838–850.

——, and ——, 1955: Some problems in optical oceanography. *J. Mar. Res.*, **14,** 63–78.

Dave, J. V., 1972: Development of programs for computing characteristics of ultraviolet radiation. Tech. Rep., Vector Case, Program V, Contract No. NAS5-21680, NASA-Goddard Space Flight Center.

Elterman, J., 1964: Parameters for attenuation in the atmospheric windows for fifteen wavelengths. *Appl. Opt.*, **3,** 745–749.

Fraser, R. S., and W. H. Walker, 1968: The effect of specular reflection at the ground on light scattered from a Rayleigh atmosphere. *J. Opt. Soc. Amer.*, **58,** 636–644.

Herman, B. M., and S. R. Browning, 1965: A numerical solution to the equation of radiative transfer. *J. Atmos. Sci.*, **22,** 559–566.

——, —— and R. J. Curran, 1971: The effect of atmosphere aerosols on the earth-atmosphere albedo. *J. Atmos. Sci.*, **32,** 1430–1445.

Kattawar, G. W., G. N. Plass and J. A. Guinn, Jr., 1973: Monte Carlo calculations of the polarization of radiation in the earth's atmosphere-ocean system. *J. Phys. Oceanogr.*, **3,** 353–372.

Mullamaa, Yu. A. R., 1964: *Atlas of the Optical Characteristics of a Disturbed Sea Surface.* Acad. Sci. Estonian SSR, 109 pp.

Plass, G. N., G. W. Kattawar and J. A. Guinn, Jr., 1975: Radiative transfer in the earth's atmosphere and ocean: influence of ocean waves. *Appl. Opt.*, **14,** 1924–36.

Quenzel, H., and M. Kaestner, 1980: Optical properties of the atmosphere: calculated variability and application to satellite remote sensing of phytoplankton. *Appl. Opt.*, **19,** 1338–1344.

Raschke, E., 1972: Multiple scattering calculation of the transfer of solar radiation in an atmosphere ocean system. *Beitr. Phys. Atmos.*, **45,** 1–19.